

Anomalous Mobility of Highly Charged Particles in Pores

² Yinghua Qiu,^{†,‡} Crystal Yang,[§] Preston Hinkle,[†] Ivan V. Vlassiouk,^{||} and Zuzanna S. Siwy^{*,†,§,⊥}

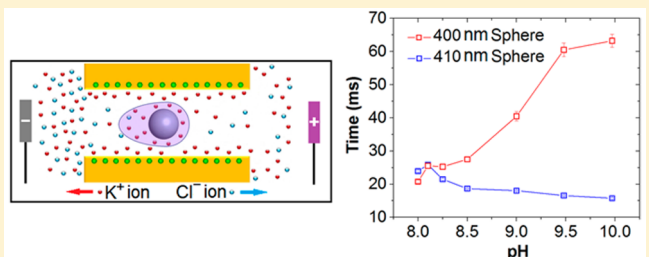
³ [†]Department of Physics and Astronomy, [§]Department of Chemistry, and [†]Department of Biomedical Engineering, University of California, Irvine, California 92697, United States

⁵ [‡]School of Mechanical Engineering and Jiangsu Key Laboratory for Design and Manufacture of Micro-Nano Biomedical Instruments, Southeast University, Nanjing 211189, China

⁷ ^{||}Oak Ridge National Laboratory, Bethel Valley Road, Oak Ridge, Tennessee 37831, United States

⁸  Supporting Information

ABSTRACT: Single micropores in resistive-pulse technique were used to understand a complex dependence of particle mobility on its surface charge density. We show that the mobility of highly charged carboxylated particles decreases with the increase of the solution pH due to an interplay of three effects: (i) ion condensation, (ii) formation of an asymmetric electrical double layer around the particle, and (iii) electroosmotic flow induced by the charges on the pore walls and the particle surfaces. The results are important for applying resistive-pulse technique to determine surface charge density and zeta potential of the particles. The experiments also indicate the presence of condensed ions, which contribute to the measured current if a sufficiently high electric field is applied across the pore.



Mobility of charged colloidal particles in electrolyte solutions has been a subject of discussion for a few decades. The discussions are stimulated by unexpected findings showing a nonmonotonic dependence of the particle mobility on its surface charge density.^{1–8} After an initial increase, when the charge density reaches a certain threshold, the mobility either saturates or starts decreasing. The effect was first described for charged polymers^{9–14} and further extended to spheres and planes.¹⁵

One explanation that was put forward is based on the deformation of the electrical double layer of counterions around a particle caused by the applied electric field.^{3,16–18} This double-layer polarization induces an additional drag force acting on the particle and consequently leads to lower particle mobility. Another explanation for the existence of maximum of the particle mobility in its dependence on the surface charge is provided by the ion condensation model.^{9,10,15,19} When the surface charge density of a polymer or particle reaches a threshold, often such that the ratio of the Bjerrum length and distance between charges exceeds 1, nearby counterions collapse on the surface reducing its zeta potential and consequently particle mobility. It is important to mention that the ion condensation model does not take into account possible influence of electric field on the structure and composition of the electrical double layer.

Here we show how passage of particles through single pores in resistive-pulse technique can elucidate the interplay between these two models and explain surface charge-dependent mobility of particles. Single pores have been used for the detection and characterization of single particles for half a century.^{20–27} Particles are observed as they pass through single

pores as a transient decrease of the current called the resistive pulse. Volume of the particles can be determined from the pulse amplitude. Electrokinetic velocity of individual particles is found from their translocation times knowing the applied voltage and pore length. Zeta potential of particles is often measured as a slope of the passage time with voltage,^{28,29} assuming faster translocations indicate higher surface charges/zeta potentials. The experiments presented here point to the necessity of performing additional measurements in order to elucidate the relationship between translocation time and surface charge density of transported objects.

Reported here resistive-pulse experiments were performed with single micrometer-sized pores and 400 nm in diameter polystyrene particles. Two types of particles contained carboxyl groups at estimated densities which differed by a factor of 6. Surface charge density of the carboxylated particles was regulated by the level of the carboxyl groups' dissociation via solution pH.¹ We found that the relative electrokinetic mobility of the two types of particles was strongly pH dependent. At pH 8, the particles with higher surface charge translocated faster than the more weakly charged particles. Increasing the pH inverted the charge-translocation time relationship, so that at pH 10 the more highly charged beads had a mobility three times lower than the mobility of the less charged beads. Inspired by earlier theoretical and numerical work on particles passage through pores,^{30–33} the results are explained by

Received: June 1, 2015

Accepted: July 16, 2015

78 interplay of (i) ion condensation and (ii) double-layer
 79 polarization, as well as (iii) electroosmosis induced by charges
 80 on the pore walls and particle surface. Electroosmotic flow
 81 caused by the charges of the translocating object was predicted
 82 before for polyelectrolytes and charged particles.^{31–35} This
 83 work shows that the electroosmotic component is also
 84 important for submicron rigid, highly charged spheres in
 85 conditions where the particle radius is ~200 times larger than
 86 the screening length.

87 ■ EXPERIMENTAL METHODS

88 **Single Pore Preparation.** Single pore membranes in two
 89 polymer materials poly(ethylene terephthalate) (PET) and
 90 polycarbonate (PC) were prepared by the track-etching
 91 technique.³⁶ Foils of 12 μm thick PET and 30 μm thick PC
 92 were first irradiated with single energetic heavy ions at the
 93 Institute for Heavy Ions Research in Darmstadt, Germany.³⁷
 94 After the irradiation, the foils were subjected to wet chemical
 95 etching, which leads to preparation of single pores whose
 96 opening diameter increases linearly with the etching time.
 97 Etchings of PET and PC pores were performed in 0.5 M
 98 NaOH, 70 °C and 5 M NaOH, 50 °C, respectively. Average
 99 diameter of etched pores was measured by recording current–
 100 voltage curves in 1 M KCl and relating the pore resistance with
 101 its geometry.^{27,38}

102 **Particles.** The particles used in the resistive-pulse experiments were purchased from Bangs Laboratories, Fisher, IN. 103 Carboxylated polystyrene particles 410 and 400 nm in diameter 104 as well as unmodified thus uncharged 400 nm polystyrene (PS) 105 particles were used in all shown measurements. The diameter 106 and surface charge densities quoted in the Article were reported 107 by the manufacturer. Zetasizer Nano ZS, Malvern Instruments 108 Ltd. was used to confirm that the diameter of the particles does 109 not significantly change with pH. It is important to mention 110 that the surface charge densities given by the manufacturer 111 should be used only in a comparative manner: surface charge 112 density of the 400 nm carboxylated particles was six times 113 higher than the surface charge density of carboxylated 410 nm 114 particles. The zeta sizer was also used to measure zeta potential 115 of the particles as a function of pH in 100 mM KCl.

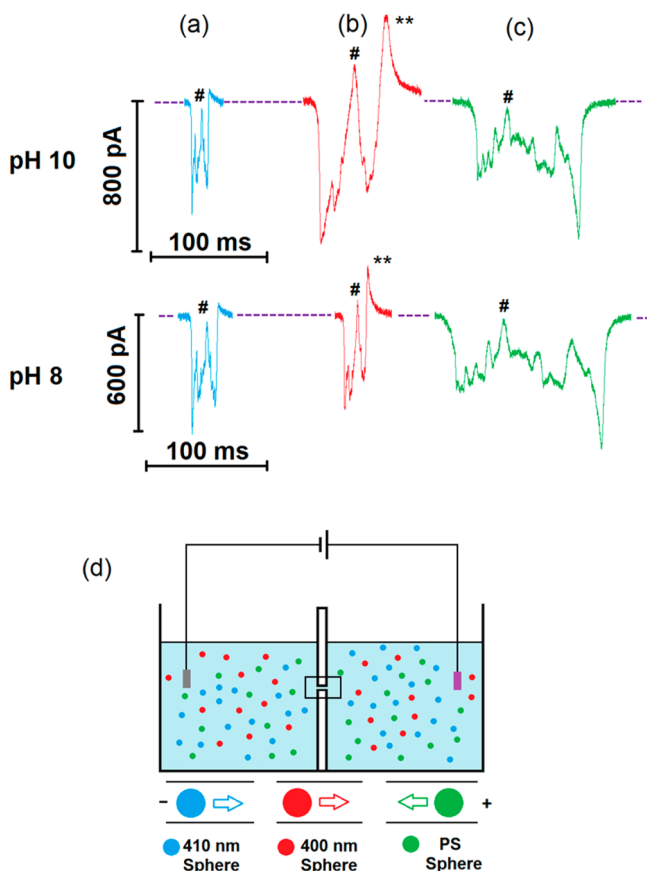
116 **Ion Current Recordings and Particle Detection.** 117 Resistive-pulse experiments were performed from suspensions 118 prepared in 100 mM KCl, with pH values ranging from 8 to 10, 119 containing 0.1% of Tween 80. The concentration of all particles 120 was $\sim 10^9$ particles/mL. Ion current measurements were 121 performed with Axopatch 200B and 1322A Digidata (Molecular 122 Devices, Inc.) using sampling frequency of 20 kHz. The 123 data were subjected to low-pass Bessel filter of 1 kHz.

124 **Comsol Modeling.** Coupled Poisson–Nernst–Planck and 125 Navier–Stokes equations were solved using the Comsol 126 Multiphysics 4.3 package.³⁹ Cylindrical pores (5 μm long) 127 were connected with 20 μm long cylindrical reservoirs; the 128 diameter of the modeled pore was 800 nm. The surface charge 129 density of the pore walls was set to $-0.25 \text{ e}/\text{nm}^2$. A very fine 130 triangular mesh of 0.1 nm was used close to the charged walls. 131 In the remaining parts of the modeled structures, the mesh was 132 reduced to the point when no change in the observed 133 concentration profiles and currents was observed upon further 134 mesh decrease. Passage of particles with surface charge density 135 of -0.25 or $-0.75 \text{ e}/\text{nm}^2$ was considered. The dielectric 136 constant of the solution $\epsilon = 80$, particle $\epsilon = 4$, and diffusion 137 coefficients $2 \times 10^{-9} \text{ m}^2/\text{s}$ were used for both potassium and 138 chloride ions. In all calculations, a potential difference of 0.1 V 139

140 was applied to the right reservoir while the left reservoir was 141 grounded.

142 ■ RESULTS AND DISCUSSION

143 Figure 1 presents resistive pulses created by three types of 144 fl particles with diameter of ~ 400 nm passing through a single 144



145 **Figure 1.** Passage of single particles through a pore with an average 146 opening diameter of 770 nm recorded at 800 mV. (a)–(c) Traces of 147 three types of particles: (a) 410 nm and (b) 400 nm in diameter 148 carboxylated polystyrene particles (marked in blue and red, 149 respectively) and (c) 400 nm unmodified/uncharged polystyrene 150 particles (green traces). The 400 nm charged particles had ~ 6 times 151 higher surface charge density than the charged 410 nm particles. (d) 152 Scheme of the conductivity cell used for the experiments. Mixture of 153 all particles was present on both sides of the membrane. The two types 154 of charged particles passed through in the direction of electrophoresis 155 (from left to right in the scheme); the uncharged particles translocated 156 in the opposite direction. The symbol # indicates the widest location 157 of the pore as traced by all particles; the dashed line marks the baseline 158 current level.

159 poly(ethylene terephthalate) (PET) pore with an average 160 opening diameter of 770 nm. Particles (410 nm) were 161 carboxylated at the reported density of 1.6 groups per 100 162 \AA^2 ; example pulses of the particles are shown in blue in Figure 163 1a. Passage of 400 nm carboxylated particles with six times 164 higher surface charge density is shown in red in Figure 1b. We 165 also present data of 400 nm unmodified polystyrene particles, 166 which passed through the pore by electroosmosis (green traces 167 in Figure 1c). In order to record passage of all particles for the 168 same voltage magnitude and voltage polarity, mixtures of the 169 particles were placed on both sides of the membrane. According to the 170 scheme in Figure 1d, the charged particles 171

157 passed through the pore from left to right; the uncharged
 158 spheres from right to left. All particles were examined in 100
 159 mM KCl with pH values between pH 8 and pH 10. pH value of
 160 the bulk electrolyte modulated the degree of deprotonation of
 161 carboxyl groups, as shown before experimentally by titration of
 162 suspensions of carboxylated polystyrene particles¹ and by
 163 molecular dynamics simulations.⁴⁰ Increasing pH from 8 to 10
 164 was shown to increase the particles' surface charge density by a
 165 factor of ~ 2 .¹

166 There are a few features of the recordings which we would
 167 like to discuss. First, the pulses of all particles are characterized
 168 by large undulations of the current. As reported by us before,
 169 the peaks and valleys of the pulses correspond to longitudinal
 170 irregularities of the pore diameter; i.e., local diameter is
 171 dependent on the axial position.^{27,41,42} This is supported by our
 172 recordings: events of the 410 nm charged particles and 400 nm
 173 uncharged polystyrene particles are a mirror image of each
 174 other due to their opposite direction of transport (Figure 1d,
 175 Figure S1). Moreover, the character of pulses of these two types
 176 of particles is independent of the solution pH, further
 177 confirming the pulses indeed reflect the pore topography;
 178 note the difference in the translocation times, which will be
 179 discussed below.

180 The pulses created by the heavily charged 400 nm particles
 181 change however with the increase of pH (Figures 1, S2). When
 182 discussing their pulses let us first point to the existence of the
 183 large current increase at the end of the particles' passage
 184 (marked as ** in Figure 1). As explained by us in our previous
 185 report, a charged particle modulates ionic concentrations at
 186 both pore entrances due to particle-induced concentration
 187 polarization.⁴³ A negatively charged particle present at the pore
 188 end in contact with a positively biased electrode increases
 189 concentration of counterions, which are sourced from this pore
 190 opening to pass through the pore; this transient increase of
 191 ionic concentrations is observed as a current increase above the
 192 baseline value, seen in our case at the end of the pulses (Figure
 193 2). Presence of the particle however also depletes local
 194 concentrations of co-ions; thus, when the particle is on the
 195 membrane side in contact with a negatively biased electrode,
 196 i.e., the side from which co-ions are sourced, an additional
 197 current decrease superimposed on the decrease caused by the
 198 excluded volume of the particle is recorded. Indeed passage of
 199 400 nm heavily charged particles starts with a current decrease
 200 whose magnitude at pH 10 exceeds the current decrease
 201 recorded at pH 8 and for other types of studied particles.

202 As suggested by the existence of a very shallow current
 203 decrease in pulses of the uncharged polystyrene particles
 204 (marked as # in Figure 1), this particular pore had a large cavity
 205 in the middle. The surprising feature of the 400 nm charged
 206 beads is that in this location at all studied pH values, the
 207 particles caused a current increase above the baseline current,
 208 especially pronounced at pH 10. One can understand this
 209 observation by treating the pore as two pores in series
 210 connected by a larger reservoir (Figure 2). The applied voltage
 211 will drop mostly over the narrower zones (regions 1 and 3 in
 212 Figure 2) so that the electric field in the wide reservoir (region
 213 2) will be the weakest. When a particle exits the first narrow
 214 zone (position 2 in Figure 2), it causes an increase of the local
 215 cation concentration, and a higher current is observed. When
 216 the particle enters the second narrow part of the pore (position
 217 3, Figure 2), anionic concentration in this position becomes
 218 depleted, and a decrease of the current is observed. Exit of the
 219 particle from the pore (position 4, Figure 2) is again

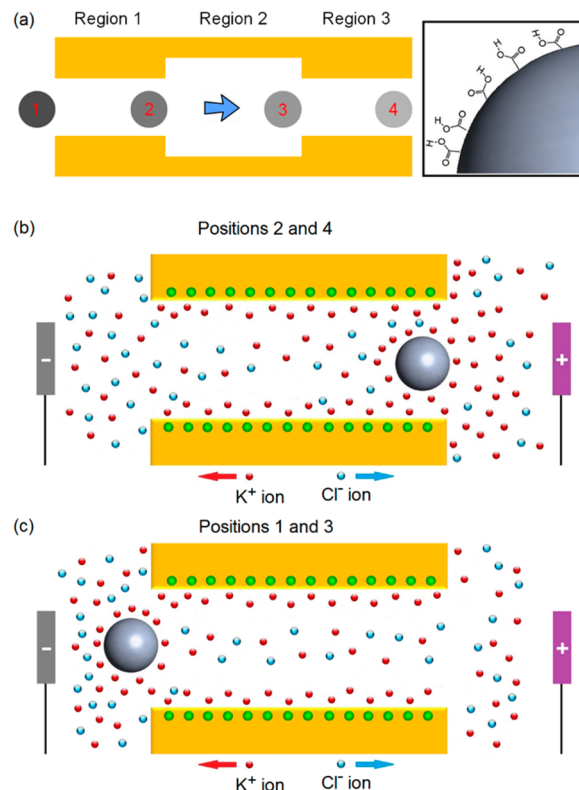


Figure 2. (a) Scheme of a pore with a large cavity in the middle and of a carboxylated particle. Presence of a negatively charged particle at pore entrances modulates local concentration of ions: it increases concentration of cations and lowers local anions concentration. (b) In positions 2 and 4, local enhancement of cation concentration causes current enhancement (# in Figure 1b corresponding to position 2, and ** to position 4), because cations are sourced from these entrances.⁴³ (c) In positions 1 and 3, depletion of anion concentration caused by the particle leads to a current decrease.

220 accompanied by a large current increase. The experiments
 221 show that highly charged particles passing through pores with
 222 undulating diameter can modify ionic concentrations in the
 223 pore to a large extent so that resolution of the pore topography
 224 by the particles is diminished.

225 Another feature of the recordings in Figure 1 is the
 226 dependence of the translocation time on the solution pH,
 227 studied in more detail in Figure 3. Behavior of 410 nm charged
 228 particles follows an expected trend: increase of pH leads to an
 229 increase of the particle surface charge density; thus, the particles
 230 translocate the fastest at pH 10 (Figure 3a, b).
 231

Properties of the translocation velocity of the 400 nm
 232 carboxylated particles are however very different. At pH 8 they
 233 translocate faster than the 410 nm particles in agreement with
 234 their higher surface charge. At solutions of higher pH, however,
 235 the passage time of the charged 400 nm particles increases
 236 drastically, and at pH 10 their translocation velocity is more
 237 than three times lower than that of the less charged particles
 238 and comparable to the velocity of uncharged particles (Figure 3
 239 d).

240 Slowing down of the highly charged particles is especially
 241 striking when studying a mixture of the particles with a pore
 242 whose opening is sufficiently large to allow for the particles to
 243 overtake each other. Figure 4 shows recordings through a 1.1
 244 μm in diameter pore in a polycarbonate (PC) film. Pulses
 245 created by the 400 and 410 nm particles can be easily
 246

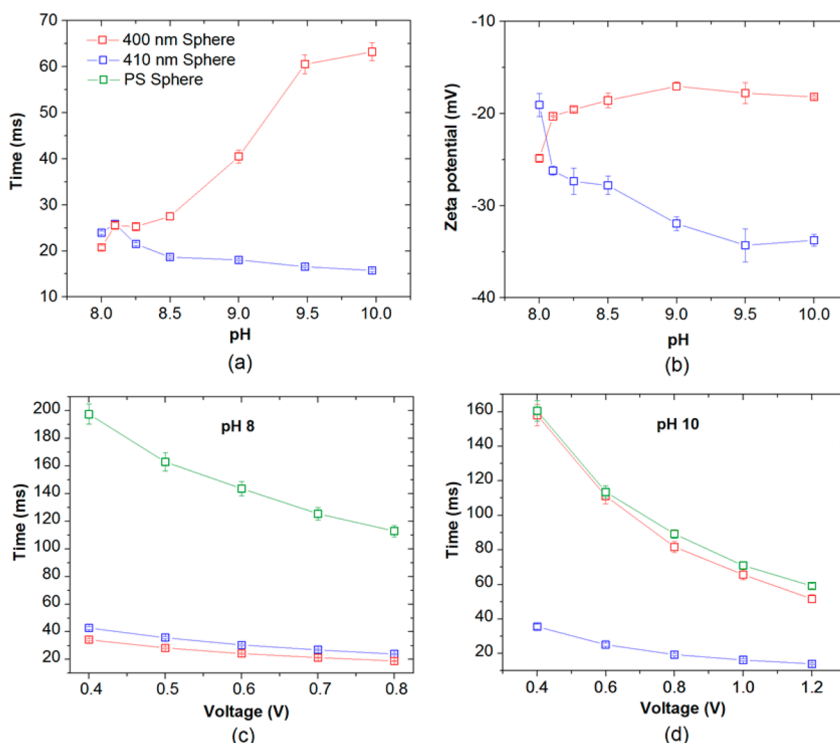


Figure 3. (a) Translocation time as a function of pH of 410 and 400 nm in diameter carboxylated particles at 800 mV. (b) Zeta potential of 410 and 400 nm particles in 100 mM KCl as a function of pH. (c), (d) Translocation times for three types of particles as a function of voltage at pH 8 (c) and pH 10 (d). The recordings were performed with a single 770 nm in diameter pore in 100 mM KCl.

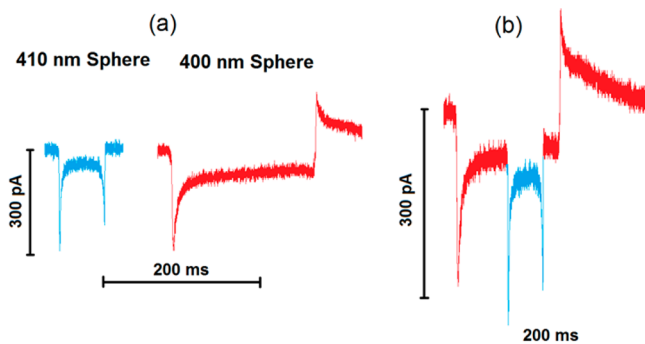


Figure 4. (a) Example ion current pulses of individual 410 and 400 nm particles passing through a single 1.1 μ m in diameter pore in a 29 μ m thick PC membrane under 1 V. (b) The fast 410 nm particle (blue trace) overtakes the slow 400 nm particle (red trace) in the pore.

246 distinguished from each other, because the more charged 400
247 nm particles produce a current increase when they exit (Figure
248 4a). Figure 4b presents a pulse in which passage of a single 400
249 nm charged particle (red trace) is interrupted by an entrance
250 and a quick exit of a 410 nm bead (blue trace). The second
251 entering particle is indeed the less charged one, because its exit
252 does not have the characteristic current increase.

253 These experiments also prompted us to ask a question
254 whether the confined volume of the micropore is sufficient to
255 reveal existence of intraparticles interactions, especially in the
256 case when the particles overtake each other. Previous
257 theoretical studies indeed revealed importance of particles'
258 charges not only in electrokinetic but also coagulation
259 processes, and stability of suspensions.^{44,45} It was shown that
260 electrostatic and/or van der Waals interactions between them
261 particles could not be neglected if the distance between them

262 was sufficiently small. If the particles interact with each other
263 when in the pore (Figure 4b), their passage time and relative
264 current change should be different from the values measured
265 when the particles translocate individually (Figure 4a). Our
266 preliminary analysis (data not shown) revealed that the 410 nm
267 particles overtaking the slower 400 nm ones do not influence
268 passage time or current blockage of either of the particles,
269 suggesting lack of interactions. In future studies, we will
270 perform similar experiments with narrower pores with
271 expectation to observe modulation of passage time and possibly
272 even *in situ* particle coagulation occurring in a pore.
273

274 Pores in PC films are known to be smooth due to amorphous
275 character of the material.⁴⁶ Thus, the recordings in Figure 4
276 indicate that the translocation of the 400 nm charged particles
277 is slowed down at pH 10 independently of the pore 3D
278 topography.
279

280 In order to explain the dependence of the passage time on
281 pH, we first measured zeta potential, ζ_{particle} , of the particles in
282 100 mM at pH between 8 and 10, as shown in Figure 3b.
283 Translocation velocity of a particle can be related with ζ_{particle}
284 via the Smoluchowski equation, taking into account zeta
285 potential of the pore, ζ_{pore} which induces electroosmotic
286 transport of the solution opposing the electrophoretic motion.⁴⁷
287

$$V_{\text{translocation}} = (\zeta_{\text{particle}} - \zeta_{\text{pore}})E/\eta$$

288 where E is the applied electric field and η solution viscosity.
289

290 Zeta potential of the 410 nm less charged particles increases
291 with pH, and consequently, the magnitude of $V_{\text{translocation}}$
292 increases as well (Figure 3a). In contrast, ζ_{particle} of the more
293 charged 400 nm particles becomes lower at higher pH values
294 and reaches a plateau at \sim pH 8.5. This saturation of ζ_{particle} with
295 surface charge can be understood via the ion condensation
296 model. It was predicted and shown experimentally that for
297

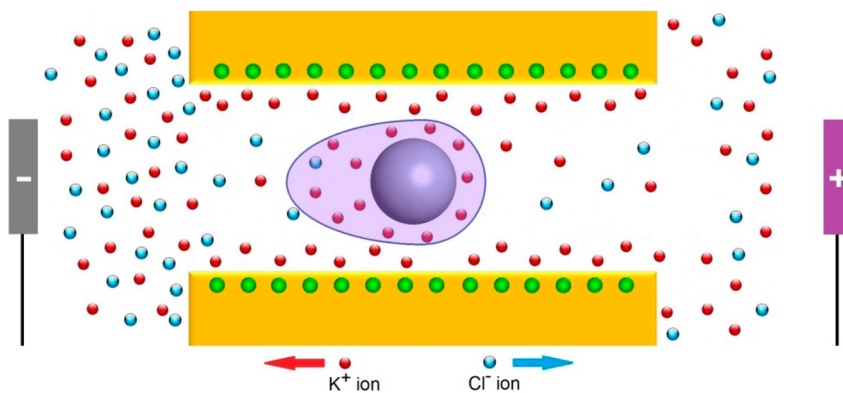


Figure 5. Scheme showing electric field induced distortion of the counterions' cloud around a moving particle.^{3,16,17,31,32}

sufficiently high surface charge densities, nearby counterions can collapse on the particle lowering the overall magnitude of ζ_{particle} as well as the number of counterions available for ionic transport.^{9,10,15} Using formulas derived by Manning,¹⁵ we confirmed that the surface charge density of the used particles estimated by the manufacturer was indeed higher than the critical value needed for ion condensation ($\sim 0.013 \text{ C/m}^2$). The measured decrease of ζ_{particle} for the 400 nm particles (Figure 3b) was however insufficient to quantitatively explain the drastic slowing down of the particles seen in Figure 3a: ζ_{particle} decreased only by a factor of 0.2 when pH was increased from pH 8 to pH 10, while the velocity decreased by a factor of 3 over the same pH interval.

Further explanation of our experimental data can be provided by the double-layer polarization, i.e., a distortion of the electrical double layer of the particles under the influence of electric field.^{3,16,17} A zone with higher ionic concentrations is created in the rear part of the particle; the front part of the particle is in contact with a zone with depleted ionic concentrations (Figure 5).^{17,31,32} The counterions' distribution was shown to exert an additional drag force, which opposes the electrophoretic transport. The model by O'Brien and White³ was derived for low external electric fields and considered zeta potential, ζ_{particle} , as the control parameter; higher surface charge density was assumed to lead to higher zeta potential values.³ The nonmonotonic dependence of the particle mobility on ζ_{particle} was explained by the quadratic dependence of the drag force on ζ_{particle} . Since the magnitude of ζ_{particle} is less than 1 V and the electrophoretic force increases with zeta potential linearly, only for sufficiently high values of ζ_{particle} does the additional drag becomes crucial for the translocation. For a particle that is 200 nm in radius moving in a solution of 100 mM KCl, the decrease of the particle mobility from its maximum value due to double-layer polarization was predicted below $\sim 40\%$.³

The counterions' cloud will become more asymmetric for particles with a higher surface charge density.^{3,31} The increase of surface charge of the highly charged 400 nm particles with pH is evidenced in our experiments by the increase of the relative amplitude of the ion current positive spike present at the end of resistive pulses (marked as ** in Figure 1). A particle with more surface charges brings a larger number of counterions which temporarily increase ionic concentrations at one of the pore entrances and increase measured ion current (Figure 6). Interestingly, the relationship of the peak magnitude with pH agrees semiquantitatively with the previously reported pH dependence of surface charge density of suspensions of

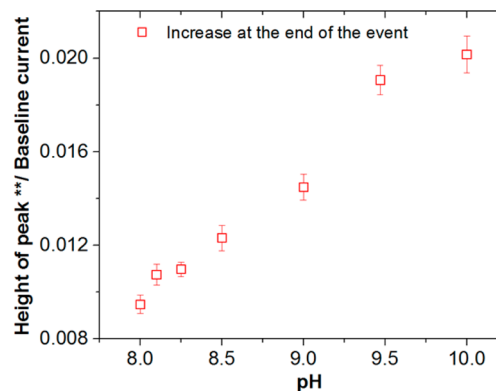


Figure 6. Relative magnitude of the current increase at the end of resistive pulses of 400 nm in diameter charged particles (marked as ** in Figure 1b) as a function of pH, at 800 mV.

carboxylated particles.¹ The relative maximum current observed experimentally (Figure 6) and the measured surface charge density (Figure 1 in ref 1) changed by a factor of 2 in the pH range between 8 and 10.

Surface charge density of the 410 nm particles is lower so that even at pH 10 the additional drag force due to counterions' cloud distortion does not lead to significant slowing down of the particles.

A combined effect of ionic condensation and polarization of electrical double layer was considered theoretically before at low applied electric fields for polyelectrolytes and particles.^{30–35} The earlier work revealed that additional effects have to be taken into account when a particle is moving through a charged pore. The particle motion will be influenced by the electroosmotic flow generated by the charged pore walls as well as charges on the moving object. For negatively charged particles and pores, electroosmosis opposes the electrophoretic translocation. Figure 7 shows numerical modeling of radial velocity profiles of a solution in the pore when a 400 nm in diameter particle is located at the pore axis. The modeling was performed by numerically solving coupled Poisson–Nernst–Planck and Navier–Stokes equations.⁴³ Computational resources restricted us to studying particles that differ in surface charge by a factor of 3, instead of the factor of 6 that our two charged, experimentally studied particles have. Two types of particles characterized by surface charge density of -0.25 and -0.75 e/ nm^2 were therefore considered. The obtained results suggest that the electroosmotic flow of solution is induced by both surface charge of the pore and surface charge of the particle,

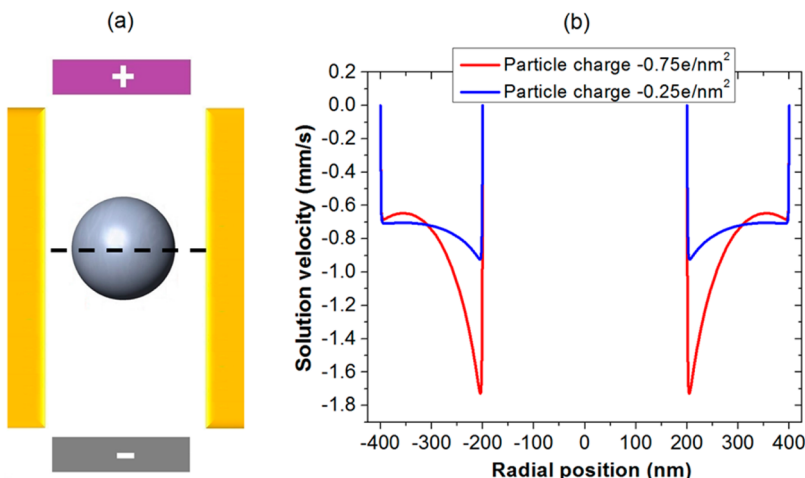


Figure 7. Numerical modeling of solution velocity in a single 5 μm long pore with diameter of 800 nm and two types of particles with surface charge density of -0.75 and -0.25 e/nm^2 , respectively. The presented solution represents radial velocity distribution along the dashed line as shown in the scheme on the left. A value of 0.1 V was applied across the pore. The surface charge density of the pore walls was set to -0.25 e/nm^2 .

369 and the more charged particles translocate slower. The
 370 predicted here effect of electroosmosis on the particle transport
 371 is more significant than reported in previous numerical
 372 studies.^{31,35} We believe the augmented electroosmotic flow
 373 shown in Figure 7 is caused by the high electric fields used in
 374 our modeling and experiments.

375 We conclude that the dramatic slowing down of the highly
 376 charged particles at pH 10 in pores is caused by a collective
 377 effect of three factors: (i) ion condensation, (ii) polarization of
 378 the particle double layer, and (iii) electroosmotic flow induced
 379 by pore walls and surface charge of the particles.

380 An interesting question however remains whether our data
 381 can reveal existence of condensed ions. The theory of ion
 382 condensation is electrostatic in nature, and we hypothesize that
 383 the externally applied voltage might be able to release some of
 384 the condensed ions, which would influence the shape of
 385 recorded resistive pulses. These electric field induced effects
 386 would not be seen in the classical experiments of zeta potential
 387 measurements since the electric fields to which the particles are
 388 subjected are low. With 1 V applied across an 11 μm long PET
 389 pore, the resulting electric field is about 100 times higher than
 390 that in a zeta sizer.

391 The effect of electric field on the number of mobile
 392 counterions can be studied by analyzing again the magnitude of
 393 the ion current increase at the end of pulses of the 400 nm in
 394 diameter particles (marked as ** in Figure 1) but this time with
 395 respect to voltage. If the number of counterions brought by the
 396 particle and available for ion transport was independent of
 397 voltage, the relative current change should also be voltage
 398 independent. Analysis of the pulses in the 770 nm pore (Figure
 399 8), and two other independently prepared pores, revealed a
 400 strong increase of the relative current increase with voltage. The
 401 data therefore suggest that the number of condensed ions
 402 might indeed be dependent on the magnitude of the external
 403 electric field.

404 ■ CONCLUSIONS

405 Resistive-pulse experiments with highly charged particles
 406 revealed a nontrivial dependence of the particles' mobility on
 407 their surface charge density. Increase of the particles' surface
 408 charge with pH can lead to significant decrease of their
 409 translocation velocity. This anomalous behavior was observed

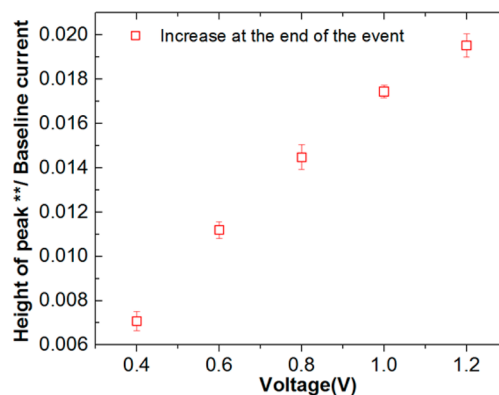


Figure 8. Relative magnitude of the current increase at the end of resistive pulses of 400 nm in diameter charged particles (marked as ** in Figure 1b) as a function of voltage, at pH 9.

with 400 nm in diameter particles whose surface contained high density of carboxyl groups. The presented experiments suggest that in order to relate mobility of particles with their zeta potential, it might be insufficient to perform experiments in only one pH solution. When studying highly charged particles, it will be necessary to compare their resistive pulses with measurements of known particles to identify potential anomalous mobility. High surface charge density of translocating particles can also be identified via the presence of a current increase above the baseline current, creating a bimodal character of a resistive pulse.^{43,44}

The experimental observation of low mobility of highly charged particles is in accordance with the double-layer polarization model, which pointed to the asymmetric character of the counterions' cloud surrounding a charged, moving particle in a solution.^{3,16,17} The results are also in agreement with previously reported numerical modeling on the importance of the double-layer polarization and ion condensation in translocation of polyelectrolytes and charged particles.^{30–32,35} The earlier models were however developed for low external electric fields, and the reported here data revealed existence of new effects at higher voltages. For example, analysis of resistive pulses provided evidence for the existence of condensed ions around the highly charged

434 particles; these ions could be released and could contribute to
435 the measured ion current in high electric fields applied across
436 the pore. It is also possible that the effect of polarization of the
437 electrical double layer on particle transport is more dominant
438 for higher external voltages. In addition, the data and modeling
439 revealed an importance of electroosmotic flow induced by the
440 charges on the pore walls as well as charges on the particles,
441 which additionally slowed down the motion of charged
442 particles. Our future experimental studies will focus on applying
443 these effects in developing new ways of separating particles by
444 their surface charge properties.

445 ■ ASSOCIATED CONTENT

446 ■ Supporting Information

447 The Supporting Information is available free of charge on the
448 ACS Publications website at DOI: [10.1021/acs.analchem.Sb02060](https://doi.org/10.1021/acs.analchem.Sb02060).

450 Experiments of particle passage at pH values between 8
451 and 10 ([PDF](#))

452 ■ AUTHOR INFORMATION

453 Corresponding Author

454 *E-mail: zsiwy@uci.edu. Tel. 949-824-8290. Fax 949-824-2174.

455 Notes

456 The authors declare no competing financial interest.

457 ■ ACKNOWLEDGMENTS

458 Irradiation with swift heavy ions was performed at the GSI
459 Helmholtzzentrum für Schwerionenforschung GmbH, Darm-
460 stadt, Germany. We very much appreciate helpful discussions
461 with Prof. Salvador Mafé from the University of Valencia in
462 Spain. This research was supported by the National Science
463 Foundation (CHE 1306058). Y.Q. acknowledges financial
464 support from the China Scholarship Council (CSC
465 201406090034).

466 ■ REFERENCES

- 467 (1) Quesada-Pérez, M.; Callejas- Fernández, J.; Hidalgo-Álvarez, R. J. *Colloid Interface Sci.* **2001**, *233*, 280–285.
- 468 (2) Fernandez-Nieves, A.; Fernandez-Barbero, A.; de las Nieves, F. J. *Langmuir* **2000**, *16*, 4090–4093.
- 469 (3) O'Brien, R. W.; White, L. R. *J. Chem. Soc., Faraday Trans. 2* **1978**, *72*, 1607–1626.
- 470 (4) Schulz, S. F.; Gisler, T.; Borkovec, M.; Sticher, H. J. *Colloid Interface Sci.* **1994**, *164*, 88–98.
- 471 (5) Martin-Molina, A.; Quesada-Perez, M.; Galisteo-Gonzalez, F.; Hidalgo-Alvarez, R. J. *Phys. Chem. B* **2002**, *106*, 6881–6886.
- 472 (6) Huang, Q. R.; Dubin, P. L.; Moorefield, C. N.; Newkome, G. R. J. *Phys. Chem. B* **2000**, *104*, 898–904.
- 473 (7) Welch, C. F.; Hoagland, D. A. *Langmuir* **2003**, *19*, 1082–1088.
- 474 (8) Guo, X.; Kirton, G. F.; Dubin, P. L. *J. Phys. Chem. B* **2006**, *110*, 20815–20822.
- 475 (9) Manning, G. S. *Acc. Chem. Res.* **1979**, *12*, 443–449.
- 476 (10) Manning, G. S. *Ber. Bunsen-Ges.* **1996**, *100*, 909–922.
- 477 (11) Shaaban, A. H.; Ander, P. *Polym. Prep.* **1993**, *34*, 970–971.
- 478 (12) Hoagland, D. A.; Smisek, D. L.; Chen, D. Y. *Electrophoresis* **1996**, *17*, 1151–1160.
- 479 (13) Popov, A.; Hoagland, D. A. *J. Polym. Sci., Part B: Polym. Phys.* **2004**, *42*, 3616–3627.
- 480 (14) Gao, J. Y.; Dubin, P. L.; Sato, T.; Morishima, Y. *J. Chromatogr. A* **1997**, *766*, 233–236.
- 481 (15) Manning, G. S. *J. Phys. Chem. B* **2007**, *111*, 8554–8559.
- 482 (16) O'Brien, R. W. *J. Colloid Interface Sci.* **1983**, *92*, 204–216.
- 483 (17) Dukhin, S. S. *Adv. Colloid Interface Sci.* **1993**, *44*, 1–134.

(18) Saville, D. A. *J. Colloid Interface Sci.* **2000**, *222*, 137–145. 494

(19) Ohshima, H. *J. Colloid Interface Sci.* **2004**, *275*, 665–669. 495

(20) Coulter, W. H. U.S. Patent 2,656,508, 1953. 496

(21) DeBlois, R. W.; Bean, C. P.; Wesley, R. K. A. *J. Colloid Interface Sci.* **1977**, *61*, 323–335. 498

(22) Berge, L. I.; Feder, J.; Jøssang, T. *Rev. Sci. Instrum.* **1989**, *60*, 499 2756–2763. 500

(23) DeBlois, R. W.; Bean, C. P. *Rev. Sci. Instrum.* **1970**, *41*, 909–916. 501

(24) DeBlois, R. W.; Wesley, R. K. *J. Virol.* **1977**, *23*, 227–233. 502

(25) Harms, Z. D.; Mogensen, K. B.; Nunes, P. S.; Zhou, K.; Hildenbrand, B. W.; Mitra, I.; Tan, Z.; Zlotnick, A.; Kutter, J. P.; Jacobson, S. C. *Anal. Chem.* **2011**, *83*, 9573–9578. 504

(26) Gear, A. R. L.; Bednarek, J. M. *J. Cell Biol.* **1972**, *54*, 325–345. 506

(27) Pevarnik, M.; Healy, K.; Toimil-Molares, M. E.; Morrison, A.; Létant, S. E.; Siwy, Z. S. *ACS Nano* **2012**, *6*, 7295–7302. 508

(28) Ito, T.; Sun, L.; Crooks, R. M. *Anal. Chem.* **2003**, *75*, 2399–2406. 509

(29) Kozak, D.; Anderson, W.; Vogel, R.; Chen, S.; Antaw, F.; Trau, M. *ACS Nano* **2012**, *6*, 6990–6997. 511

(30) Hsu, J.-P.; Chen, Z.-S.; Tseng, S. *J. Phys. Chem. B* **2009**, *113*, 7701–7708. 513

(31) Yeh, L.-H.; Hsu, J.-P. *Soft Matter* **2011**, *7*, 396–411. 515

(32) Hsu, J.-P.; Tai, Y.-H.; Yeh, L.-H.; Tseng, S. *J. Phys. Chem. B* **2011**, *115*, 3972–3980. 517

(33) Zhang, M.; Ai, Y.; Kim, D.-S.; Jeong, J.-H.; Joo, S. W.; Qian, S. *Colloids Surf., B* **2011**, *88*, 165–174. 518

(34) Luan, B.; Aksimentiev, A. *Phys. Rev. E* **2008**, *78*, 021912. 520

(35) Zhang, X.; Hsu, J.-P.; Chen, Z.-S.; Yeh, L.-H.; Ku, M.-H.; Tseng, S. *J. Phys. Chem. B* **2010**, *114*, 1621–1631. 521

(36) Fleischer, R. L.; Price, P. B.; Walker, R. M. *Nuclear Tracks in Solids: Principles and Applications*; University of California Press: Berkeley, CA, 1975. 523

(37) Spohr, R. German Patent DE 2 951 376 C2, U.S. Patent 4 369 370, 1983. 526

(38) Apel, P.; Korchev, Y. E.; Siwy, Z.; Spohr, R.; Yoshida, M. *Nucl. Instrum. Methods Phys. Res., Sect. B* **2001**, *184*, 337–346. 528

(39) Vlassiouk, I.; Smirnov, S.; Siwy, Z. S. *Nano Lett.* **2008**, *8*, 1978–1985. 530

(40) Schwierz, N.; Horinek, D.; Netz, R. R. *Langmuir* **2015**, *31*, 215–225. 532

(41) Pevarnik, M.; Schiel, M.; Yoshimatsu, K.; Vlassiouk, I. V.; Kwon, J. S.; Shea, K. J.; Siwy, Z. S. *ACS Nano* **2013**, *7*, 3720–3728. 534

(42) Innes, L.; Chen, C.-H.; Schiel, M.; Pevarnik, M.; Haurais, F.; Tomil-Molares, M. E.; Vlassiouk, I. V.; Theogarajan, L.; Siwy, Z. S. *Anal. Chem.* **2014**, *86*, 10445–10453. 536

(43) Menestrina, J.; Yang, C.; Schiel, M.; Vlassiouk, I.; Siwy, Z. S. *J. Phys. Chem. C* **2014**, *118*, 2391–2398. 539

(44) Hidalgo-Alvarez, R.; Martin, A.; Fernandez, A.; Bastos, D.; Martinez, F.; de las Nieves, F. J. *Adv. Colloid Interface Sci.* **1996**, *67*, 1–118. 541

(45) Felix, C.; Yaroshchuk, A.; Pasupathi, S.; Pollet, B. G.; Bondarenko, M. P.; Kovalchuk, V. I.; Zholkovskiy, E. K. *Adv. Colloid Interface Sci.* **2014**, *211*, 77–92. 544

(46) Müller, S.; Schötz, C.; Picht, O.; Sigle, W.; Kopold, P.; Rauber, M.; Alber, I.; Neumann, R.; Toimil-Molares, M. E. *Cryst. Growth Des.* **2012**, *12*, 615–621. 547

(47) Schoch, R. B.; Han, J.; Renaud, P. *Rev. Mod. Phys.* **2008**, *80*, 839–883. 551

(48) Lan, W.-J.; Kubeil, C.; Xiong, J.-W.; Bund, A.; White, H. S. *J. Phys. Chem. C* **2014**, *118*, 2726–2734. 552